Hindawi Publishing Corporation
Advances in Materials Science and Engineering
Volume 2016, Article ID 1430641, 12 pages
http://dx.doi.org/10.1155/2016/1430641

Research Article

Effect of Temperature on Permeability and Mechanical Characteristics of Lignite

Jixi Shao, Yaoqing Hu, Tao Meng, Su Song, Peihua Jin, and Gan Feng

Institute of Mining Technology, Taiyuan University of Technology, Taiyuan 030024, China

Correspondence should be addressed to Yaoqing Hu; huyaoqing163@163.com

Received 9 September 2016; Accepted 2 November 2016

Academic Editor: Patrice Berthod

Underground in situ pyrolysis and gasification is an important method to enable clean utilization of lignite in China. In this study, using the high-temperature triaxial permeability test equipment for different ranges of temperature and pore pressure, the permeability and mechanical characteristics of lignite from the Pingzhuang Mine Area in Chifeng have been examined. The results show that, at constant confining pressure, the elastic modulus of lignite decreases with increasing temperature. For temperature up to approximately 75°C, the elastic modulus is close to the modulus under the uniaxial state. As the temperature increases, the stress-strain curves during loading and unloading are different. The differences between the curves during loading and unloading are greater at higher temperature due to the greater residual deformation. In addition, in different temperature ranges (i.e., 150–650°C), the triaxial creep curves of lignite are different. In particular, at 300–450°C, the triaxial creep curve of lignite alternates between the accelerated creep and the steady creep. Moreover, the permeability change rule in the lignite is complex, and it is governed by the temperature and pore pressure. Hence, for different temperature range and pore pressure, the variations in the permeability are different. In fact, as the temperature increases, the permeability of lignite fluctuates.

1. Introduction

Lignite accounts for a large proportion of coal reserves in China. According to the national coal resources survey, the proven reserve of lignite is 131.142 billion tons. This is 13% of the total coal reserve (1.00326 trillion tons) in China [1]. However, due to its high oxygen content, spontaneous combustion of lignite can easily occur. Together with its high moisture content, lignite is difficult to store. Further, as there is a high content of volatile matter in lignite and due to its relatively low heat content, when lignite is burned for power generation, it usually leads to serious air pollution. Therefore, research studies in China have focused on efficient and clean utilization of lignite resource. They found that one of the most effective ways is underground pyrolysis and gasification.

Coal pyrolysis and gasification is a process in which coal, which is heated to a high temperature in the absence of air, goes through physical and chemical changes to generate pyrolysis products, such as coal gases (CH_4, H_2, and CO_2), liquid (tar), and solid (coke) [2, 3]. In the process of underground coal pyrolysis and gasification, gas is required to permeate into an outlet pipe through surrounding coal and rock masses [4]. However, if gas fails to permeate into the outlet pipe smoothly, it may diffuse and permeate into other surrounding rock masses, thereby causing environmental pollution [5, 6]. During the process of coal pyrolysis and gasification, the movement of gas is mainly governed by the permeability and mechanical characteristics of the surrounding coal and rock masses.

Permeability and mechanical characteristics of coal are affected by many factors, such as pore, matrix shrinkage [7], temperature, effective stress, and pore pressure [8], and there are many reports on the effect of pore and fracture on coal permeability. Previous researchers concluded that, for the pores and fractures that are larger and better connected, there is higher coal permeability [9–17].

The effects of temperature and stress on coal permeability are more complex. By carrying out the methane permeating test with briquette at 50°C, Cheng et al. [18] developed an expression relating the temperature and stress to coal permeability. Yang and Zhang [19] studied the variation of coal seam gas permeability with changing temperature

under gas-solid coupling. They found that, at the low effective stress, the effect of temperature on the permeability is significant, but, at the high effective stress, the effect is small. Li et al. [20] conducted an experimental study on the coal permeability under different temperature and stress. Their results showed that, at the low effective stress, the coal permeability increases with increasing temperature, but, at the high effective stress, it decreases with increasing temperature. However, the maximum temperature of 70°C was still not up to the temperature required for coal pyrolysis (i.e., 200°C) [21]. Hu et al. [13] conducted an experiment to study the effects of the temperature and stress on the permeability characteristics of briquette and raw coal. The maximum temperature was 250°C. They found that there is an exponential relationship between the permeability of the briquette and raw coal and the confining stress under the pressurized and depressurized conditions. Feng et al. [22] conducted permeability experiments from room temperature to 600°C with gas coal and anthracite. The results showed that, during the process, there is a threshold temperature in which the permeability changes with changing temperature. Further, the threshold temperature is dependent on the degree of coal metamorphism.

Hu et al. [23] studied the effects of various factors on the permeability of lignite, including the temperature, volume stress, and pore pressure. The results showed that there are three scenarios. For constant temperature and pore pressure, the permeability decreases with increasing volume stress. For constant temperature and volume stress, the permeability first decreases then increases with increasing pore pressure, and the threshold pore pressure is 2 MPa. For constant volume stress and pore pressure, the changes in the permeability are more complex. For this scenario, as the temperature increases, the permeability of lignite first decreases and reaches a minimum at 50°C. Then, the permeability increases and reaches a maximum at 80°C. Thereafter, it decreases again.

Liu et al. [4] studied the variation of the permeability for temperature below 400°C. They found that the permeability of lignite is relatively high at around 50°C and at a minimum at 200°C–300°C. Above 300°C, the permeability of lignite increases with increasing temperature. Akbarzadeh and Chalaturnyk [24] summarized the research findings on the effect of the temperature on the coal permeability. The review focuses on the structural changes of coal with variation in temperature during the process of underground gasification.

Niu et al. [25] found that, with the pore pressure increasing from 0.5 MPa to 1.5 MPa, the coal permeability decreases under low pore pressure. They then posed the following question: what is the effect of the pore pressure on the coal permeability if the pore pressure continues to increase? To answer this question, in this study, the effect of the pore pressure from 0.5 MPa to 5.0 MPa on the lignite permeability has been investigated.

Hitherto, there are few studies on the effect of temperature on the mechanical properties (i.e., elastic modulus and creep) of lignite. Yang et al. [26] studied the elastic modulus and creep behaviors of lignite below 80°C and found that the duration of the steady creep at 80°C is shorter than that at 50°C. In detail, they found that the steady creep lasted for 160 min at 80°C, and then it turned into the accelerated creep. On the other hand, the steady creep lasted for as long as 450 min at 50°C before it turned into the accelerated creep. Ma et al. [27] conducted an experimental study to investigate the variation of mechanical properties from 25°C to 300°C. The results showed that the variations in the coal strength, elastic modulus, and the strain can be divided into four temperature ranges. First, from 25°C to 50°C, with increasing temperature, the coal strength and elastic modulus decrease, and the strain increases. Then, from 50°C to 100°C, the coal strength and elastic modulus decrease, and the strain decreases. Next, from 100°C to 200°C, the coal strength and elastic modulus increase and the strain increases. Finally, from 200°C to 300°C, the coal strength and elastic modulus decrease and the strain continues to increase.

Figure 1: Lignite specimen for the permeability test.

In this study, the permeability and mechanical properties (i.e., uniaxial compression strength, triaxial compression strength, and creep) of lignite from China's Pingzhuang Mine Area have been investigated for the temperature range from 20°C to 650°C and the pore pressure range from 0.5 MPa to 5 MPa. The objective of this study is to determine the variations of the permeability and mechanical properties of lignite during the process of underground gasification.

2. Experiments

2.1. Coal Sample Preparation. Lignite coal samples (Figure 1) were obtained from the Pingzhuang Mine Area in China's Chifeng. They were processed into four standard test coal samples (100 mm high × 50 mm in diameter). Of the four samples, one was used to conduct uniaxial stress-strain test at 20°C, and the other three were used for the creep and permeability tests.

In order to avoid coal cracking due to the existence of air, the samples were placed in a vacuum drying chamber at 40°C. The results of the proximate and ultimate analyses of

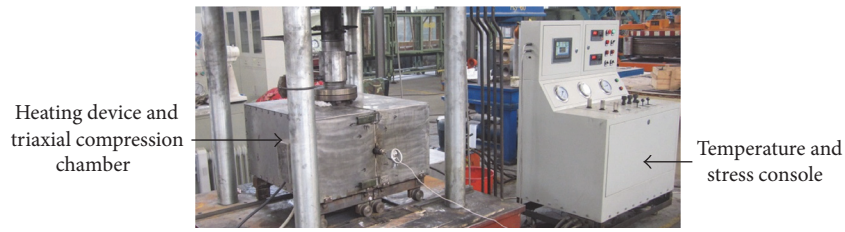

Figure 2: Photograph of high-temperature triaxial permeability test equipment.

Table 1: Results of proximate and ultimate analyses of the dried lignite specimen.

Proximate analysis (wt%)				Ultimate analysis (wt%)				
M	V	A	FC	C	H	O	N	S
18.36	26.72	20.41	34.51	50.74	3.23	12.37	1.48	1.36

Note: M, moisture content; V, volatile matter; A, ash; FC, fixed carbon.

the lignite are shown in Table 1, which show that the lignite specimens are high in volatile, ash, and moisture contents and medium in sulfur content.

2.2. Experimental Test Equipment. A self-designed high-temperature and high-pressure triaxial stress permeability test system, as shown in Figure 2, has been used as the test equipment. It can provide a maximum axial stress of 25 MPa, a maximum confining stress of 30 MPa , and a maximum pore pressure of 20 MPa, which correspond to the in situ condition at the depth of 1,000 m. As for the equipment, the most important feature is the high-temperature graphite packing, which plays a vital role in transferring the confining stress and sealing the sample. This is because the graphite packing has not only the feature of high-temperature resistance but also good elasticity which enables the confining stress to be transferred under high temperature and high stress. As for the permeable medium gas, it goes through the sample from the bottom of the equipment and discharges through the central hole of the strut to the measuring equipment of the gas flow. The heating furnace has been used as the heating equipment, and the temperature control system has been used for temperature control. Figure 3 shows schematic diagram of the test system.

2.3. Experimental Method. The flow chart in Figure 4 shows the test procedures. A standard sample was placed in the triaxial stress permeability equipment. The axial stress and the confining stress were both increased to 8 MPa and kept constant for a period of time.

In order to obtain the triaxial stress-strain curve of the lignite coal sample at 20°C, the axial stress was slowly increased to 12 MPa with the confining stress remaining constant at 8 MPa. Then, the axial stress was slowly decreased to 10 MPa, corresponding to in situ condition of 400 m buried depth and a coefficient of lateral stress of 0.8.

The triaxial stress-strain tests of the lignite coal sample at 50°C, 75°C, and 100°C were conducted at the axial stress ranging from 10 MPa to 12 MPa and the confining stress at 8 MPa.

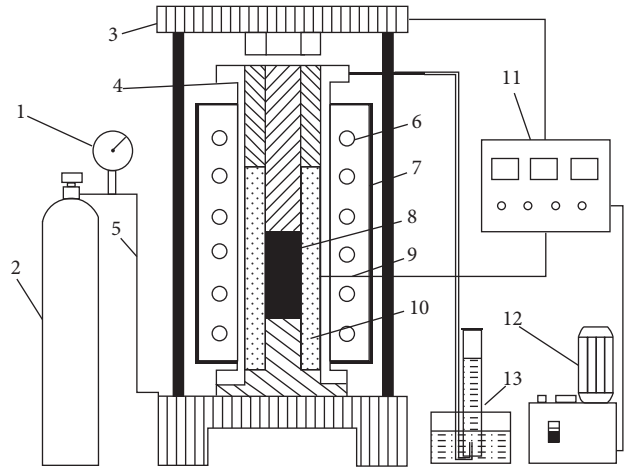

Figure 3: Schematic diagram of high-temperature triaxial permeability testing system: (1) pressure gauge, (2) nitrogen tank, (3) support frame, (4) steel tube, (5) valve, (6) heating wire, (7) muff, (8) specimen, (9) thermocouple, (10) graphite packing, (11) temperature and pressure controller, (12) oil pump, and (13) measuring equipment of gas flow.

The creep tests were conducted from 150°C to 650°C with a temperature gradient of 50°C under the triaxial stress (i.e., at the axial stress of 10 MPa and the confining stress of 8 MPa). The details of the method are as follows. First, the temperature was increased to a predetermined value. Then, the pyrolysis of coal sample took place and the products (gases) were discharged through the outlet of the permeability test equipment. When the gases stopped discharging through the outlet, the process of pyrolysis was considered over. Then, the permeability test started, in which the creep deformation was observed continuously for four hours and the triaxial creep curve was obtained.

The permeability test was carried out using nitrogen before each mechanical test (i.e., the triaxial stress-strain test or the creep test). The test temperature ranged from 20°C to 650°C, and the pore pressure ranged from 0.5 MPa to 5 MPa, increasing at a step of 0.5 MPa. The heating rate was 5°C/min. The temperature was kept constant for four hours after each triaxial stress-strain test (i.e., 50°C, 75°C, and 100°C). At each creep testing temperature, the specimens were held for four hours. When there were no more chemical and physical reactions in the permeability tests, the experimental precision was considered satisfied.

Table 2: Elastic moduli of lignite at different temperatures.

Temperature (°C)	Elastic modulus (MPa)			
	1#	2#	3#	average
20	888.89	1000.00	800.00	896.30
50	526.32	666.67	416.67	536.55
75	506.34	528.32	370.37	468.34
100	285.71	285.71	240.96	270.79

3. Results and Discussions

3.1. Stress-Strain Behavior of Lignite at Different Temperatures under Uniaxial and Triaxial Conditions. In order to compare and analyze the deformation features of lignite under different uniaxial and triaxial stress states, the stress-strain curves from the experiments at different temperatures and stress conditions have been examined. The uniaxial stress-strain curve of lignite at 20°C is shown in Figure 5. Figures 6, 7, and 8 show, respectively, the triaxial stress-strain curve of lignite samples 1#, 2#, and 3# at different temperatures.

3.1.1. Relationships between Elastic Modulus and Temperature. The elastic modulus at different temperature and average elastic modulus of the three coal samples are listed in Table 2. It is apparent that the elastic modulus decreases with increasing temperature. At 75°C, the average elastic modulus of 468.34 MPa is close to the elastic modulus of 472.98 MPa under the uniaxial state. However, at 100°C, the average elastic modulus decreases to 270.79 MPa. Even for the different degrees of coal metamorphism and stress state, these results are similar to those of the earlier studies [27–29]. The elastic modulus decreases with increasing temperature mainly due to the volatile components in the coal, which have higher rates of evaporation at the higher temperature. This is particularly true for lignite as it contains high moisture content. The higher temperature causes the moisture to evaporate and thermal cracking in the lignite. The strength and elastic modulus therefore become lower. In this experiment, the temperature range is from 20°C to 100°C, within which pyrolysis normally does not occur. Therefore, elastic modulus decreases mainly due to the volatile components volatilizing and water evaporating.

3.1.2. Stress-Strain Curve Characteristics. The uniaxial and triaxial stress-strain curves of lignite at 20°C (Figures 6–8) are similar to those of the rock-like materials [30]. The results show that the triaxial stress-strain curves are different during loading and unloading, which is an indication that the coal is a hysteretic material. The elastic modulus of lignite under the triaxial stress is twice as that under the uniaxial stress. Under the triaxial stress, the deviation degree between the loading and unloading curves increases with increasing temperature, which is an indication that the residual deformation is greater at the higher temperature. This is because as the temperature rises, more of the volatile components in lignite evaporate, thereby causing thermal cracking in the lignite. As the stress increases, fractures close up, but when the stress decreases, the closed fractures do not open again, thereby resulting in the residual deformation.

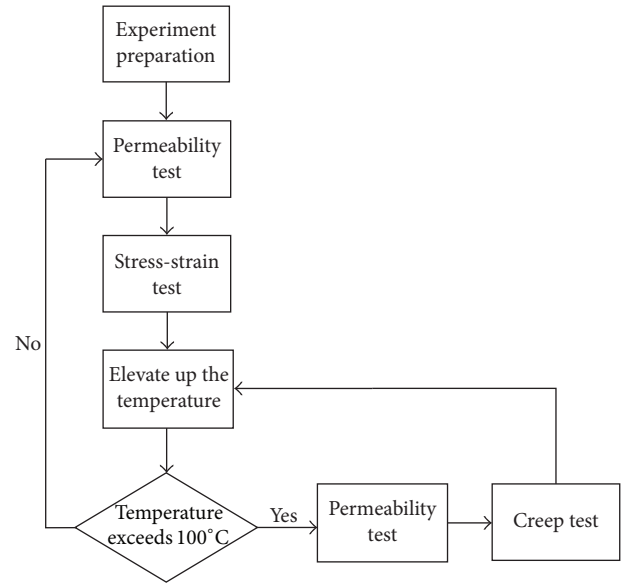

Figure 4: Flow chart diagram of the test procedure.

Figures 6, 7, and 8 show the changes in the strain in the triaxial stress-strain curves when the axial stress increases from 8 MPa to 12 MPa at 20°C and from 10 MPa to 12 MPa at 50, 75, and 100°C. Due to the limited range of the stress variations, the curves only show partial stress-strain characteristics. In addition, except for the stress-strain curve at 20°C, the stress-strain curves at the other temperatures have been obtained under the special circumstance. That is, the permeability tests were first conducted at the predetermined temperatures using nitrogen. Then, the stress-strain tests were conducted after the completion of the permeability experiments when the pore pressure was zero. During the permeability test experiment, nitrogen removed the volatile components in the samples, especially when the temperature reached 100°C. This temperature caused the volatilization to accelerate, resulting in an increase in deformation and a decrease in the elastic modulus.

3.2. Triaxial Stress Creep Characteristics of Lignite at Different Temperatures. In this study, the effect of temperature (i.e., ranging from 150°C to 650°C) on the creep characteristics of lignite samples 1#, 2#, and 3# has been investigated. All the samples show almost the same creep trends versus temperature. Hence, only one of the samples has been selected for further discussion. The typical triaxial creep curves of the coal sample between 150°C and 650°C are shown in Figure 9.

3.2.1. Creep Characteristics in Low-Temperature Range (150°C–250°C). As shown in Figure 9, the creep curves at 150°C, 200°C, and 250°C are basically similar. Further, the creep deformation gradually increases steadily with time. This is because, at temperature of 250°C and below, the pyrolysis

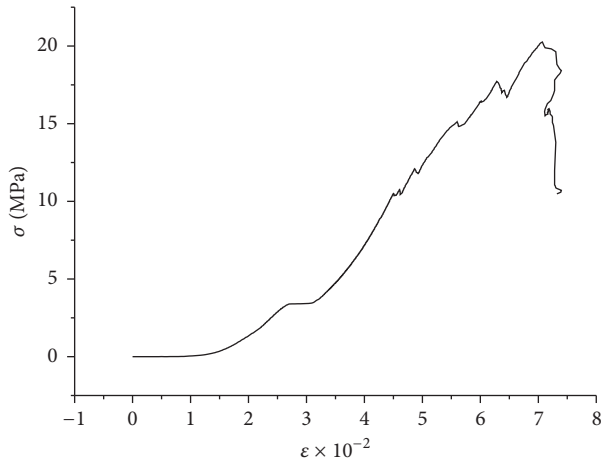

Figure 5: Uniaxial stress-strain curve of lignite at 20°C.

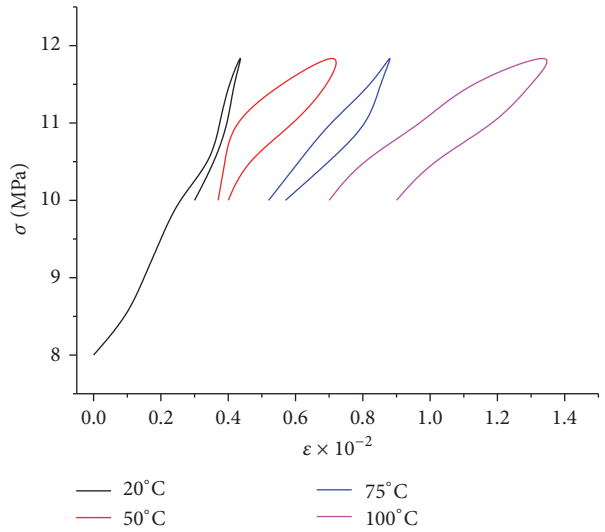

Figure 6: Triaxial stress-strain curves of coal sample 1# at different temperatures.

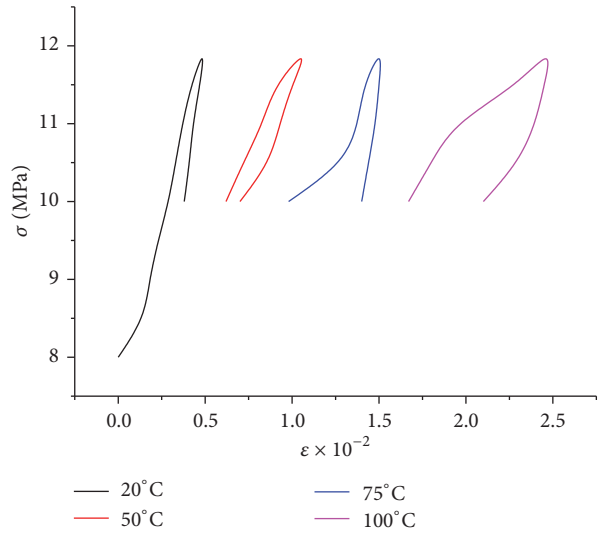

Figure 7: Triaxial stress-strain curves of coal sample 2# at different temperatures.

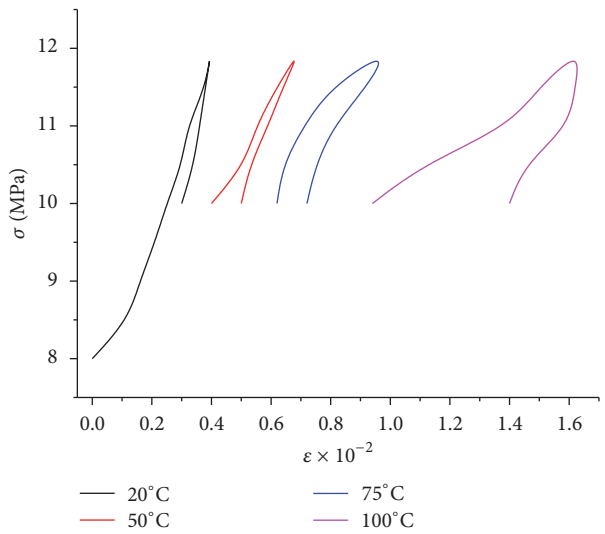

Figure 8: Triaxial stress-strain curves of coal sample 3# at different temperatures.

reaction of coal is relatively slow, and only volatile components including moisture discharge [31]. Under the triaxial stress, pores and fractures close quickly and the coal skeleton remains basically intact. Hence, the creep is steady and the coal can take a range of loadings.

3.2.2. Creep Characteristics in Moderate-Temperature Range (300°C–450°C). As shown in Figure 9, the creep curves at 300°C, 350°C, 400°C, and 450°C are slightly different. There are two processes, the steady creep and the accelerated creep, alternating. These processes are due to the occurrence of lignite pyrolysis within this temperature range. The pyrolysis products (gas and tar) are generated, which create substantial amounts of pores, cavities, and fractures in the coal. At the same time, the steady creep of the lignite samples under the triaxial stress is also occurring. Then, when the creep deformation reaches a critical value, irreversible damage of the coal skeleton occurs. During this process, the creep rate (i.e., the slope of curve) suddenly increases, which is known as the accelerated creep. The pores, voids, and fractures within the coal sample have been compacted. Then, the compressive capacity of the coal increases, thereby reducing the deformation. At the same time, the creep rate reduces, which is shown as the steady creep. Similarly, when the creep deformation reaches a critical value, the pores, voids, and fractures are compacted and some are even closed, which is shown as the accelerated creep followed by the steady creep. Normally, these processes repeat several times.

3.2.3. Creep Characteristics in High-Temperature Range (500°C–650°C). As shown in Figure 9, creep deformation increases significantly between 500°C and 650°C, which is mainly shown as the accelerated creep. On the other hand, the creep curves fluctuate within a small range. This

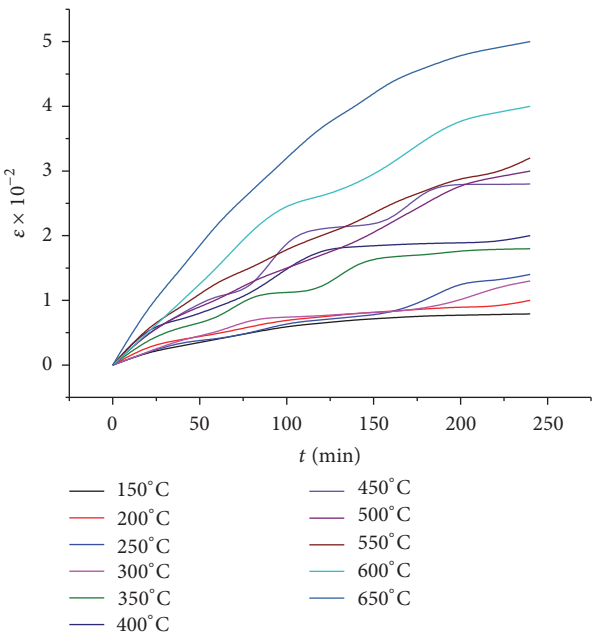

Figure 9: Triaxial creep curves of coal sample between 150°C and 650°C.

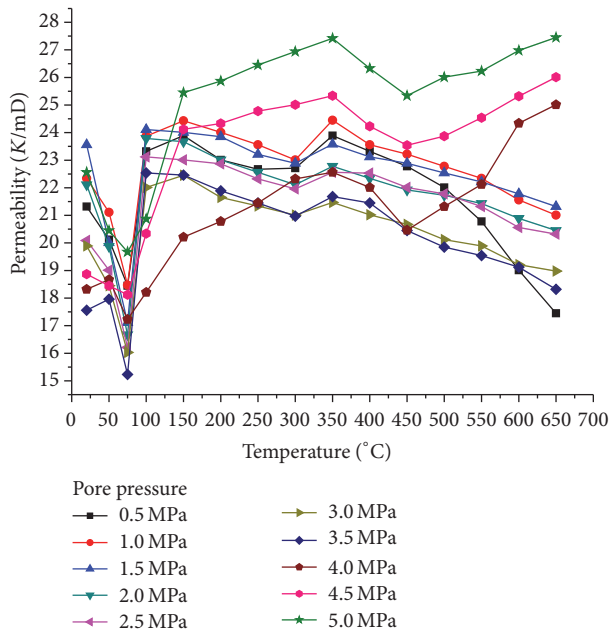

Figure 10: Variations of permeability of lignite at different temperatures and pore pressures.

is because, within this temperature range, the pyrolysis of coal is more intensive as compared to those in the lower temperature ranges. The skeleton of coal sample is softened under the high temperature. There are no clear boundaries between the pores and fractures. In fact, it turns into a pore network structure. Therefore, the plastic deformation that has occurred over time under the stress is relatively unstable, resulting in the accelerated creep.

3.2.4. Analysis of Deformation Characteristics during Lignite Pyrolysis. Under the condition of constant stress, as the temperature increases, the pyrolysis of the lignite starts to appear gradually. During this process, the degree of pyrolysis varies with temperature, resulting in different deformation characteristics. This experimental study shows that, during the process, elasticity, plasticity, and rheology are the main features of lignite deformation. For the deformation below 100°C, it is mainly elastic deformation. For the deformation above 100°C, it is mainly plastic and rheological deformations. Moreover, as the temperature increases, pyrolysis products increase, resulting in a large number of voids in the coal. As the coal is subjected to the stress condition, the stress softens the coal, resulting in plastic and rheological deformations. Further, at higher temperature, the degree of deformation is greater. Hence, the plastic deformation has been mainly caused by the pyrolysis process, and, after a period of time, the rheological deformation started. Due to the limitations of the experiment, the rheological deformation only lasted for 4 h. At the end of the experiment, the average height of the three test samples has shortened by 37 mm, and the average weight has decreased by 53%.

In fact, during the process of gasification and pyrolysis, the pyrolysis area expands with the duration of the process. If the coal is subjected to the stress of surrounding rock all the time, during the pyrolysis of the coal, both the size of the coal and the passage of the permeation become smaller, resulting in a smaller gasification rate. On the other hand, the experimental results show that the pyrolysis of the coal under the low stress not only increases the pyrolysis rate but also improves the transfer efficiency of the pyrolysis products.

3.3. Permeability Characteristics of Lignite at Different Temperatures and Pore Pressures. This experimental study focuses on the effect of the pore pressure and the temperature on the permeability of lignite under the fixed stresses (i.e., axial stress of 10 MPa and confining stress of 8 MPa). The average data of the three samples have been used to calculate the permeability. The permeability has been calculated using the following equation [20]:

$$K = \frac{2\mu p_0 Q_0 L}{\left(p_1^2 - p_2^2\right) A}, \quad (1)$$

where μ is the dynamic viscosity of nitrogen (1.8×10^{-5} Pa·s); L is the height of the sample (cm); p_1 is the inlet pressure (Pa); p_2 is the outlet pressure (Pa); Q_0 is the flow rate (cm^3/s); and p_0 is the atmospheric pressure.

Table 3 shows the calculated permeability under different temperatures and pore pressures.

3.3.1. Relationships between Lignite Permeability and Temperature. Figure 10 shows the variations of permeability of lignite at different temperatures and pore pressures. Based on the pore pressure range, the change in permeability with temperature can be divided into three categories.

Category I: Low Pore Pressure Range (0.5 MPa–2 MPa). Figure 11 shows the relationship between permeability and pore

Table 3: Permeability at different temperatures and pore pressures.

T	p	K
20	0.5	21.32
	1	22.34
	1.5	23.56
	2	22.11
	2.5	20.09
	3	19.89
	3.5	17.56
	4	18.32
	4.5	18.87
	5	22.56
50	0.5	20.12
	1	21.11
	1.5	20.01
	2	19.87
	2.5	19.01
	3	18.45
	3.5	16.96
	4	18.67
	4.5	18.45
	5	20.45
75	0.5	18.45
	1	18.47
	1.5	17.11
	2	16.67
	2.5	16.21
	3	16.03
	3.5	15.23
	4	17.23
	4.5	18.12
	5	19.67
100	0.5	23.32
	1	23.87
	1.5	24.11
	2	23.79
	2.5	23.12
	3	21.78
	3.5	22.54
	4	18.21
	4.5	20.34
	5	20.87
150	0.5	23.89
	1	24.43
	1.5	24.01
	2	23.67
	2.5	23.01
	3	22.45
	3.5	22.10
	4	20.21
	4.5	24.12
	5	25.45
200	0.5	23.01
	1	24.01
	1.5	23.85
	2	23.01
	2.5	22.87
	3	21.65
	3.5	21.45
	4	20.78
	4.5	24.33
	5	25.87
250	0.5	22.67
	1	23.56
	1.5	23.21
	2	22.56
	2.5	22.32
	3	21.34
	3.5	21.12
	4	21.45
	4.5	24.78
	5	26.45
300	0.5	22.71
	1	23.01
	1.5	22.89
	2	22.11
	2.5	21.96
	3	21.01
	3.5	20.97
	4	22.32
	4.5	25.01
	5	26.94
350	0.5	23.89
	1	24.45
	1.5	23.58
	2	22.78
	2.5	22.56
	3	21.47
	3.5	21.32
	4	22.56
	4.5	25.34
	5	27.42
400	0.5	23.32
	1	23.56
	1.5	23.12
	2	22.34
	2.5	22.53
	3	21.02
	3.5	20.89
	4	22.01
	4.5	24.23

Table 3: Continued.

T	p	K
	5	26.33
450	0.5	22.78
	1	23.22
	1.5	22.89
	2	21.92
	2.5	22.01
	3	20.67
	3.5	20.45
	4	20.46
	4.5	23.54
	5	25.34
500	0.5	22.01
	1	22.78
	1.5	22.54
	2	21.73
	2.5	21.78
	3	20.12
	3.5	19.85
	4	21.32
	4.5	23.87
	5	26.01
550	0.5	20.78
	1	22.34
	1.5	22.21
	2	21.43
	2.5	21.32
	3	19.89
	3.5	19.54
	4	22.12
	4.5	24.54
	5	26.23
600	0.5	19.01
	1	21.56
	1.5	21.78
	2	20.89
	2.5	20.56
	3	19.21
	3.5	19.12
	4	24.34
	4.5	25.32
	5	26.98
650	0.5	17.45
	1	21.01
	1.5	21.32
	2	20.45
	2.5	20.32
	3	18.98
	3.5	18.32
	4	25.01
	4.5	26.01
	5	27.45

Note: T, temperature (°C); p, pore pressure (MPa); K, permeability (mD).

pressure ranging from 0.5 MPa to 2 MPa. It can be seen that permeability fluctuates several times from high to low as the temperature increases. The variation of permeability is different at different temperature range, and the trends can be divided into five stages.

Stage One (Temperature between 20°C and 75°C). As shown in Figure 11, when the temperature is below 75°C, permeability

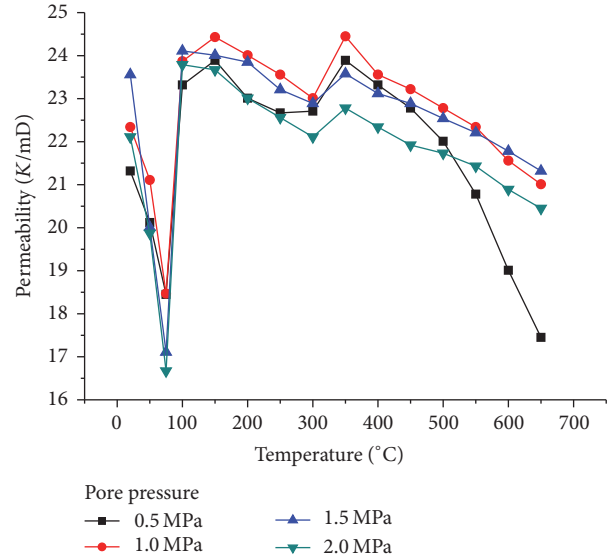

Figure 11: Variations of permeability with temperature (category I).

decreases with increasing temperature. This is because as the temperature increases, the coal expands due to the heat, thereby closing the pores and fractures that previously existed. The permeable channels also become smaller by the combined effect of the thermal stress and the volume stress, resulting in lower permeability. Therefore, within this temperature range, the permeability of coal decreases abruptly as the temperature increases.

Stage Two (Temperature between 75°C and 150°C). In this temperature range, the permeability increases with increasing temperature. This is because as the temperature increases, the moisture and some volatile components are exuded [32–35]. This phenomenon can be confirmed by the off-gas in the outlet. Evaporation of the water induces thermal cracking of the lignite and thus induces more permeable channels, leading to an increase in permeability. In this temperature range, the pyrolytic reaction of lignite is very weak. In view of this, evaporation of water and volatilization of volatile components are the major causes for the increase in permeability. The permeability reaches the first peak (i.e., 24.43 mD) at the temperature of 150°C and the pore pressure of 1 MPa.

Stage Three (Temperature between 150°C and 300°C). In this temperature range, the pyrolysis of lignite starts to take place. Due to the discharge of pyrolysis products, a large number of pores and fractures are formed. Consequently, there are more permeable channels in the lignite. On the other hand, the coal goes soft during the pyrolysis process. Hence, the permeable channels close again due to the combined effect of the confining pressure and the thermal expansion. Within this temperature range, the number of closed seepage channels is more than the number generated by the pyrolysis process. Overall, the number of permeable channels is less.

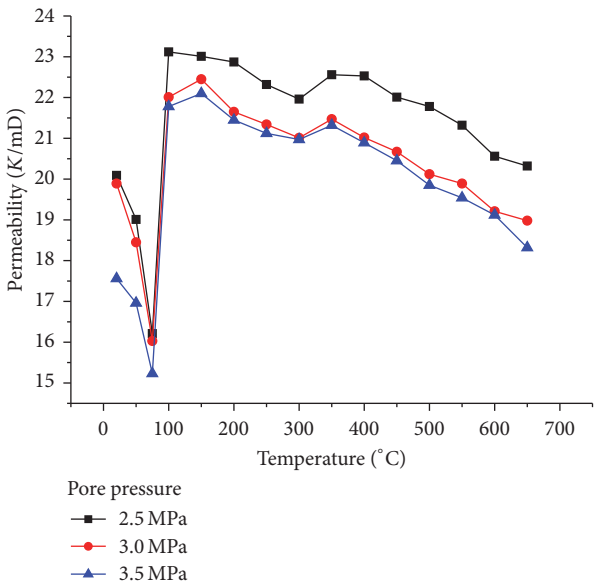

Figure 12: Variations of permeability with temperature with pore pressure ranging from 2.5 to 3.5 MPa (category II).

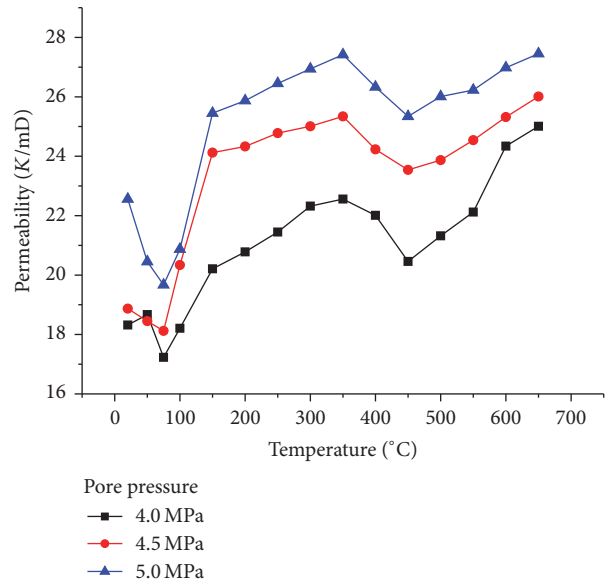

Figure 13: Variations of permeability with temperature (category III).

The lignite permeability therefore decreases with increasing temperature.

Stage Four (Temperature between 300°C and 350°C). In this temperature range, the pyrolysis of lignite continues, resulting in an increase in the pyrolysis gas products as compared to Stages 1–3 [32–34], which creates more permeable channels. On the other hand, due to the stress, permeable channels are being closed. However, the number of channels being closed is less than the number of new channels created. Overall, there are more permeable channels. Therefore, within this temperature range, permeability increases with increasing temperature. The permeability reaches the second peak (24.45 mD) at the temperature of 350°C.

Stage Five (Temperature between 350°C and 650°C). In this temperature range, drastic depolymerization and polycondensation reactions occur in the coal mass [32–34]. Many gas products (H_2, CO, CO_2, C_mH_n, etc.) discharge. The existing partial pores and fractures are blocked by the plastic mass formed by the softening and melting of the coal, resulting in a lower permeability. More importantly, due to the softening of the lignite, the bearing capacity of the structural frame of the lignite becomes weaker. Therefore, the coal mass is severely compacted under triaxial stress, and the interconnected pores inside the coal are closed, resulting in a lower permeability.

Category II: Moderate Pore Pressure Range (2.5 MPa–3.5 MPa). Figure 12 shows the relationships between the permeability and temperature with pore pressures ranging from 2.5 MPa to 3.5 MPa. From Figure 12, it can be seen that the relationships are substantially similar to those in Category I.

Category III: High Pore Pressure Range (4 MPa-5 MPa). Figure 13 shows the relationships between the permeability and temperature with pore pressures ranging from 4 MPa to 5 MPa. The variations can be divided into five stages according to the temperature ranges. At the first stage (20°C–75°C) and the second stage (75°C–150°C), the variations of the permeability are similar to those in Categories I and II. However, at the third stage (150°C–350°C), the permeability increases slowly, which is different from those in Categories I and II. In this temperature range, due to the increase in pore pressure and the reduction in the number of closed permeable channels after pyrolysis, the effective stress on the coal decreases [36–40]. Ultimately, there are more permeable channels. Therefore, within this temperature range, permeability increases with increasing temperature. At the fourth stage (350°C–450°C), despite the constant effective stress, the coal continues to be pyrolyzed and new permeable channels are created. Meanwhile, the rising temperature further softens the coal. When the strength of the coal can no longer resist the effective stress, the volume of the coal skeleton becomes smaller, thereby closing the permeable channels. Therefore, within this temperature range, permeability decreases with increasing temperature. At the fifth stage (450°C–650°C), generally, the permeability increases gradually with increasing temperature. Within this temperature range, new permeable channels are created by the coal pyrolysis. During the pyrolysis process, one part of the permeable channels is closed under stress, while the other part becomes effective permeable channels. Ultimately, there are more effective permeable channels at the higher temperature. Therefore, within this temperature range, permeability increases with increasing temperature.

Comparison between the Permeability and the Pore Volume and Specific Surface Area. Permeability measurement at a pore pressure of 5 MPa at different temperatures was repeated

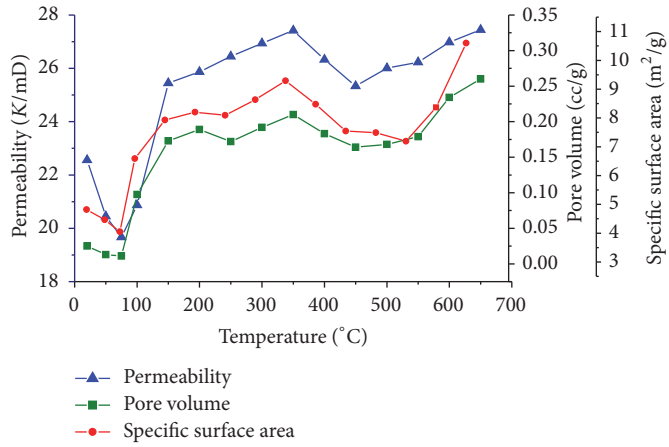

Figure 14: Variation of the permeability, specific surface area, and pore volume with temperature.

to prepare the heated lignite specimen for nitrogen adsorption experiments. The nitrogen adsorption experiments were carried out using the BUILDER 3H-2000PS2 physical adsorption analyzer. In order to satisfy the experimental requirements (i.e., nitrogen adsorption experiments), the postexperiment specimens were carefully broken down into small chunks. Then, by using the Brunauer-Emmett-Teller formula and the Barrett-Joyner-Halenda method, the specific surface area and pore volume of heated specimens were obtained, as shown in Figure 14.

As can be seen from Figure 14, the effect of temperature on the specific surface area and pore volume of heated specimen is very strong. Overall, the variation trend of specific surface area and pore volume has been shown to be significantly consistent with the results of permeability. In the temperature range of 20–75°C, specific surface area and pore volume decreased dramatically with the increase of temperature. From 75 to 150°C, the specific surface area and pore volume increase dramatically with the increase of temperature. However, slow increases in specific surface area and pore volume are observed from 150 to 350°C. Subsequently, in the temperature range of 350–550°C, due to the closure of porosity and fracture, the permeability of specimens slowly decreased with the increase of temperature. As mentioned above, in this stage, the coal specimens became so soft that large deformations were generated under the action of the triaxial stress, resulting in the closure of the pores and fractures. As the pores and fractures were closed, the penetration of the nitrogen was obstructed, resulting in a lower permeability. From 550 to 650°C, the specific surface area and pore volume dramatically increased with the increase of temperature. In summary, according to the experimental results, it can be concluded that the variation trend of the permeability is mainly due to the change of the porosity. And the porosity is positively correlated with the permeability.

3.3.2. Relationships between Lignite Permeability and Pore Pressure. Based on the data in Table 3, Figure 15 shows the relationships between the permeability and pore pressure at different temperatures. Some of the data in Table 3 are not shown in Figure 15 because the curves from these data are similar to those in Figure 15.

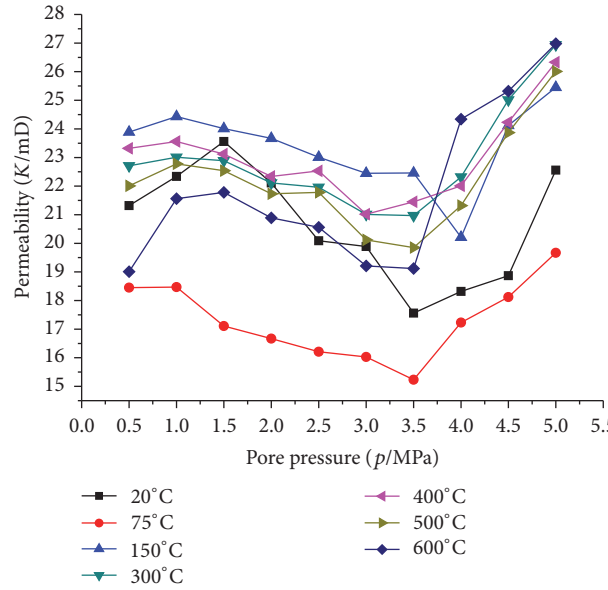

Figure 15: Variations of permeability with pore pressure at different temperatures.

From Figure 15, it can be seen that, at each temperature, the variations of the permeability with pore pressure are essentially similar. The change in permeability can be divided into three stages.

Stage I (0.5 MPa~1 MPa). For the pore pressure less than 1 MPa, the permeability increases with increasing pore pressure. At this stage, the pore pressure is relatively low, which is insufficient to cause coal deformation; that is, there is no effect on the existing pores and fractures. Therefore, the higher the pore pressure, the higher the permeability.

Stage II (1 MPa~3.5 MPa). At this stage, the permeability decreases with increasing pore pressure. Due to the increasing pore pressure, the pores and fractures in the coal matrix change. On one hand, due to the increasing pore pressure,

some closed pores and fractures are opened up. On the other hand, the previous opened pores and fractures are being closed again. The expansion of the coal skeleton induced by increasing pore pressure is less than the shrinkage resulting from the confining stress. Ultimately, there are less open permeable channels. Therefore, permeability decreases with increasing pore pressure.

Stage III (3.5 MPa~5 MPa). At this stage, the permeability increases with increasing pore pressure. This is due to the reduction in the effective volume stress caused by the increasing pore pressure [36, 37, 40]. As the pore pressure dominates at this stage, the pores and fractures opened up again. Ultimately, there are more open permeable channels. Therefore, permeability increases with increasing pore pressure.

4. Conclusions

In this study, the relationships between the mechanical and permeability characteristics of lignite coal and temperature have been investigated.

The experimental results show that, at constant confining pressure, the elastic modulus of lignite decreases with increasing temperature. For temperature up to approximately 75°C, the elastic modulus is close to the modulus under the uniaxial state. As the temperature increases, the stress-strain curves show different states; that is, the stress-strain curves are different during loading and unloading. Due to the greater residual deformation, the higher the temperature is, the larger the differences are.

Triaxial creep properties of lignite vary at different temperature ranges. For the temperature less than 250°C, the steady creep dominates. For the temperature between 300°C and 450°C, the creep curves alternate between the accelerated creep and the steady creep. For the temperature between 500°C and 650°C, the creep deformation rapidly increases, which is mainly the accelerated creep.

The variation of lignite permeability is affected by temperature and pore pressure. This study shows that the permeability of lignite fluctuates with increasing temperature. Moreover, the fluctuation in the permeability is dependent on the pore pressure.

Competing Interests

The authors declare that they have no competing interests.

Acknowledgments

The experiment has been supported by National Natural Science Foundation of China (Grant no. 51574173) and Shanxi Province Research Fund of Science and Technology for Youth (2015021120).

References

[1] L. Q. Yin, "Lignite resources and utilization outlook in China," *Coal Science and Technology*, vol. 8, pp. 12–14, 2004 (Chinese).

[2] D. B. Anthony and J. B. Howard, "Coal devolatilization and hydrogastification," *AIChE Journal*, vol. 22, no. 4, pp. 625–656, 1976.

[3] A. Arenillas, F. Rubiera, J. J. Pis et al., "Thermal behaviour during the pyrolysis of low rank perhydrous coals," *Journal of Analytical and Applied Pyrolysis*, vol. 68-69, pp. 371–385, 2003.

[4] S. Q. Liu, S. J. Zhang, F. Chen, C. H. Wang, and M. Y. Liu, "Variation of coal permeability under dehydrating and heating: a case study of ulanqab lignite for underground coal gasification," *Energy and Fuels*, vol. 28, no. 11, pp. 6869–6876, 2014.

[5] M. J. Humenick and C. F. Mattox, "Groundwater pollutants from underground coal gasification," *Water Research*, vol. 12, no. 7, pp. 463–469, 1978.

[6] K. Kapusta, K. Stańczyk, M. Wiatowski, and J. Chećko, "Environmental aspects of a field-scale underground coal gasification trial in a shallow coal seam at the Experimental Mine Barbara in Poland," *Fuel*, vol. 113, pp. 196–208, 2013.

[7] A. K. Verma and A. Sirvaiya, "Comparative analysis of intelligent models for prediction of Langmuir constants for CO_2 adsorption of Gondwana coals in India," *Geomechanics and Geophysics for Geo-Energy and Geo-Resources*, vol. 2, no. 2, pp. 97–109, 2016.

[8] M. S. A. Perera, P. G. Ranjith, S. K. Choi, A. Bouazza, J. Kodikara, and D. Airey, "A review of coal properties pertinent to carbon dioxide sequestration in coal seams: with special reference to Victorian brown coals," *Environmental Earth Sciences*, vol. 64, no. 1, pp. 223–235, 2011.

[9] Y. Q. Hu, Y. S. Zhao, and D. Yang, "Relationship between permeability and fractal dimension of coal mass," *The Chinese Journal of Mechanical Engineering*, vol. 21, no. 10, pp. 1452–1456, 2002 (Chinese).

[10] J. J. Liu and X. G. Liu, "The effect of effective pressure on porosity and permeability of low permeability porous media," *International Journal of Geomechanics*, vol. 7, no. 1, pp. 41–44, 2001 (Chinese).

[11] Y. S. Zhao, F. Qu, Z. J. Wan, Y. Zhang, W. G. Liang, and Q. R. Meng, "Experimental investigation on correlation between permeability variation and pore structure during coal pyrolysis," *Transport in Porous Media*, vol. 82, no. 2, pp. 401–412, 2010.

[12] Z.-J. Wan, Z.-J. Feng, Y.-S. Zhao, Y. Zhang, G.-W. Li, and C.-B. Zhou, "Elastic modulus's evolution law of coal under high temperature and triaxial stress," *Journal of the China Coal Society*, vol. 36, no. 10, pp. 1736–1740, 2011 (Chinese).

[13] X. Hu, W. Liang, S. J. Hou, X. Zhu, and W. Huang, "Experimental study of effect of temperature and stress on permeability characteristics of raw coal and shaped coal," *Chinese Journal of Rock Mechanics and Engineering*, vol. 31, no. 6, pp. 1222–1229, 2012 (Chinese).

[14] C. E. Salmas, A. H. Tsetsekou, K. S. Hatzilyberis, and G. P. Androutsopoulos, "Evolution lignite mesopore structure during drying. Effect of temperature and heating time," *Drying Technology*, vol. 19, no. 1, pp. 35–64, 2001.

[15] D. Jasinge, P. G. Ranjith, X. Choi, and J. Fernando, "Investigation of the influence of coal swelling on permeability characteristics using natural brown coal and reconstituted brown coal specimens," *Energy*, vol. 39, no. 1, pp. 303–309, 2012.

[16] S. Durucan and J. S. Edwards, "The effects of stress and fracturing on permeability of coal," *Mining Science and Technology*, vol. 3, no. 3, pp. 205–216, 1986.

[17] V. Vishal, T. N. Singh, and P. G. Ranjith, "Influence of sorption time in CO2-ECBM process in Indian coals using coupled numerical simulation," *Fuel*, vol. 139, pp. 51–58, 2015.

[18] A. Arenillas, F. Rubiera, J. J. Pis et al., "Thermal behaviour during the pyrolysis of low rank perhydrous coals," *Journal of Analytical and Applied Pyrolysis*, vol. 68, pp. 371–385, 2003.

[19] X. L. Yang and Y. L. Zhang, "Experimental study of effect of temperature on coal gas permeability under gas-solid coupling," *Journal of Geomechanics*, vol. 4, article 7, 2008 (Chinese).

[20] Z.-Q. Li, X.-F. Xian, and Q.-M. Long, "Experiment study of coal permeability under different temperature and stress," *Journal of China University of Mining and Technology*, vol. 38, no. 4, pp. 523–527, 2009 (Chinese).

[21] E. M. Suuberg, W. A. Peters, and J. B. Howard, "Product composition and kinetics of lignite pyrolysis," *Industrial & Engineering Chemistry Process Design and Development*, vol. 17, no. 1, pp. 37–46, 1978.

[22] Z. J. Feng, Z. J. Wan, Y. S. Zhao et al., "Experimental study of permeability of anthracite and gas coal masses under high temperature and triaxial stress," *Chinese Journal of Rock Mechanics and Engineering*, vol. 29, no. 4, pp. 689–696, 2010 (Chinese).

[23] Y. Hu, Y. Zhao, D. Yang, and Z. Kang, "Experimental study of effect of temperature on permeability characteristics of lignite," *Chinese Journal of Rock Mechanics and Engineering*, vol. 29, no. 8, pp. 1585–1590, 2010 (Chinese).

[24] H. Akbarzadeh and R. J. Chalaturnyk, "Structural changes in coal at elevated temperature pertinent to underground coal gasification: a review," *International Journal of Coal Geology*, vol. 131, pp. 126–146, 2014.

[25] S. W. Niu, Y. S. Zhao, and Y. Q. Hu, "Experimental ivestigation of the temperature and pore pressure effect on permeability of lignite under the in situ condition," *Transport in Porous Media*, vol. 101, no. 1, pp. 137–148, 2014.

[26] Y. Yang, D. H. Han, Y. M. Yu, and Y. Q. Hu, "Experimental study on thermal deformation characteristics of lignite," *Journal of Taiyuan University of Technology*, vol. 41, no. 2, pp. 201–204, 2010 (Chinese).

[27] Z. G. Ma, X. B. Mao, Y. S. Li, Z. Q. Chen, and P. Zhu, "Experimentation research on influence of temperature on coal's mechanical properties," *Ground Pressure and Strata Control*, vol. 22, no. 3, pp. 46–48, 2005.

[28] J. X. Zhou, G. L. Wang, and Z. J. Shao, "Coal deformation under high temperature and confining pressure," *Journal of China Coal Society*, vol. 19, no. 3, pp. 324–332, 1994 (Chinese).

[29] B. Jiang, Y. Qin, and F. L. Jin, "Coal deformation test under high temperature and confining pressure," *Journal of China Coal Society*, vol. 22, no. 1, pp. 80–84, 1997 (Chinese).

[30] J. C. Jaeger, N. G. Cook, and R. Zimmerman, *Fundamentals of Rock Mechanics*, John Wiley & Sons, New York, NY, USA, 2009.

[31] J. F. Xi, J. Liang, X. C. Sheng, L. X. Shi, and S. Li, "Characteristics of lump lignite pyrolysis and the influence of temperature on lignite swelling in underground coal gasification," *Journal of Analytical and Applied Pyrolysis*, vol. 117, pp. 228–235, 2016.

[32] L. Zou, L. J. Jin, X. L. Wang, and H. Q. Hu, "Pyrolysis of Huolinhe lignite extract by in-situ pyrolysis-time of flight mass spectrometry," *Fuel Processing Technology*, vol. 135, pp. 52–59, 2015.

[33] Q. Q. He, K. J. Wan, A. Hoadley, H. Yeasmin, and Z. Y. Miao, "TG–GC–MS study of volatile products from Shengli lignite pyrolysis," *Fuel*, vol. 156, pp. 121–128, 2015.

[34] H. Y. Meng, S. Z. Wang, L. Chen, Z. Q. Wu, and J. Zhao, "Thermal behavior and the evolution of char structure during co-pyrolysis of platanus wood blends with different rank coals from northern China," *Fuel*, vol. 158, pp. 602–611, 2015.

[35] Y. Xu, Y. Zhang, Y. Wang, G. Zhang, and L. Chen, "Gas evolution characteristics of lignite during low-temperature pyrolysis," *Journal of Analytical and Applied Pyrolysis*, vol. 104, pp. 625–631, 2013.

[36] J. Xu, J. Cao, B. B. Li, T. Zhou, M. H. Li, and D. Liu, "Experimental research on response law of permeability of coal to pore pressure," *Chinese Journal of Rock Mechanics and Engineering*, vol. 32, no. 2, pp. 225–230, 2013 (Chinese).

[37] J. P. Tang, Y. S. Pan, C. Q. Li, Q. Shi, and Z. X. Dong, "Experimental study on effect of effective stress on desorption and seepage of coalbed methane," *Chinese Journal of Rock Mechanics and Engineering*, vol. 25, no. 8, pp. 1563–1568, 2006 (Chinese).

[38] G. Z. Yin, X. S. Li, H. B. Zhao, X. Q. Li, and X. F. Jing, "Experimental study of effect of gas pressure on gas seepage of outburst coal," *Chinese Journal of Rock Mechanics and Engineering*, vol. 28, no. 4, pp. 697–702, 2009.

[39] H. Siriwardane, I. Haljasmaa, R. McLendon, G. Irdi, Y. Soong, and G. Bromhal, "Influence of carbon dioxide on coal permeability determined by pressure transient methods," *International Journal of Coal Geology*, vol. 77, no. 1-2, pp. 109–118, 2009.

[40] D. Jasinge, P. G. Ranjith, and S. K. Choi, "Effects of effective stress changes on permeability of latrobe valley brown coal," *Fuel*, vol. 90, no. 3, pp. 1292–1300, 2011.